

## TRANSITIONS AMONG FIVE POLYMORPHS OF CHLORPROPAMIDE NEAR THE MELTING POINT

V. A. Drebuschak<sup>1,2\*</sup>, Tatiana N. Drebuschak<sup>1,3</sup>, N. V. Chukanov<sup>1,4</sup> and Elena V. Boldyreva<sup>1,3</sup>

<sup>1</sup>Novosibirsk State University, Ul. Pirogova 2, Novosibirsk 630090, Russia

<sup>2</sup>Institute of Geology and Mineralogy SB RAS, Pr. Ak. Koptiyuga, 3, Novosibirsk 630090, Russia

<sup>3</sup>Institute of Solid State Chemistry and Mechanochemistry, SB RAS, Kutateladze 18, Novosibirsk, 630128 Russia

<sup>4</sup>Novosibirsk Institute of Organic Chemistry, SB RAS, Pr. Ak. Lavrentieva, 9, Novosibirsk, 630090 Russia

Five polymorphs of chlorpropamide ( $\alpha$ ,  $\beta$ ,  $\gamma$ ,  $\delta$ , and  $\epsilon$ ) were investigated near the melting point by using DSC. Structure of samples was tested by X-ray powder diffraction. Four first polymorphs were found to transform into  $\epsilon$ -polymorph, which melts at  $T_m=128^\circ\text{C}$ ,  $\Delta_m H=24\text{ kJ mol}^{-1}$ . Enthalpy of the polymorph transitions ranges from  $+3\text{ kJ mol}^{-1}$  for  $\alpha\rightarrow\epsilon$  to  $-0.8\text{ kJ mol}^{-1}$  for  $\beta\rightarrow\epsilon$ .

Structure of three first polymorphs was published elsewhere, and the structure of  $\delta$ -polymorph is published for the first time. XRPD patterns for all polymorphs are reported, together with the atomic coordinates for the  $\delta$ -polymorph.

**Keywords:** calorimetry, chlorpropamide, polymorphs, structure

### Introduction

Chlorpropamide,  $\text{C}_{10}\text{H}_{13}\text{ClN}_2\text{O}_3\text{S}$ , is used as a drug that treats type II (noninsulin-dependent) diabetes. In pharmaceutical research, it is used as a model for the investigation of drug-excipient interaction in order to increase the bioavailability of a drug with low solubility in water in a pure form.

Several polymorphs of chlorpropamide were reported so far. They were characterized by X-ray powder diffraction, differential thermal analysis, IR spectroscopy, dissolution rate measurements, and others. In sum, we found out the information about 16 polymorphs of chlorpropamide. Thirteen entries were collected in the Powder Diffraction Files database (PDF-50). Three other X-ray diffraction patterns were taken from [1], not included in the database. Polymorphs in [1] were named A, B and C. XRPD patterns in the PDF-50 were taken from [2] (five entries: 34-1877, 34-1878, 34-1879, 34-1881 and 34-1882, enumerated from I to V) and [3] (seven entries: from 35-1966 to 35-1972). One entry is a private communication (H. Rose, Eli Lilly and Co., Indianapolis, Indiana, USA). It is interesting that the printed version of [2] contains only four XRPD patterns, from I to IV.

Unfortunately, information about all these polymorphs, plenty in number, cannot be considered reliable, because the data were reported in a way that does not allow one to identify the polymorphs correctly: X-ray powder diffraction results were shown on figures or in tables with interplanar spaces and intensities, but without  $hkl$  indexes and unit cell

parameters. Even the total number of chlorpropamide polymorphs is unknown, in fact, so far. For example, it was not defined which polymorph denoted by a letter in [1] corresponds to a polymorph denoted by a Roman numeral in [2].

Now it is common to use letters A (starting material), B (after melting) and C (after polymorph transition) for chlorpropamide polymorphs [1, 4, 5], but too often published X-ray powder diffraction patterns for chlorpropamide samples denoted by the same letter differ from one another.

Procedure of a sample preparation (heating, melting, solving, etc.) is usually described in pharmaceutical reports on chlorpropamide instead of structural data (unit cell parameters). The products (polymorphs) are considered to be always identical after identical preparations. Unfortunately, this is not true. It is well known that the same preparation yields too often different polymorphs [6], the same polymorph is prepared after different procedures, and sometimes the synthesis of polymorphs cannot be reproduced never again [7]. To be sure which polymorph is dealt this time with, one should necessarily define its structure. At long last, only the structure is the criterion for the identification of any polymorph [8, 9].

Only one orthorhombic polymorph of chlorpropamide was known to exist with certainty for a long time. Its structure is described in the Cambridge Structural Database as entry BEDMIG [10, 11]. Recently we solved the structure of two new chlorpropamide polymorphs,  $\beta$  [12] and  $\gamma$  [13]. Structure of a new polymorph ( $\delta$ ) was solved, but not

\* Author for correspondence: dva@xray.nsu.ru

reported yet. As for the last polymorph ( $\varepsilon$ ), recently 'a proposed crystal structure' for it was solved from powder X-ray diffraction, but, unfortunately, neither cif-file nor atomic coordinates were reported [14].

Objective of this work is to report the transitions among five polymorphs of chlorpropamide at heating. The DSC experiments were supported by the XRPD control of starting materials and products. Such a combination of experimental techniques yields the information very useful for the characterization of both materials and pharmaceutical process [15].

## Experimental

### Samples

The polymorphs are denoted with Greek letters in order of structure solution. The relation between polymorphs denoted by Greek and Roman letters is approximately as follows: A= $\alpha$ , B= $\beta$ , and C= $\varepsilon$ . This relation is not exact because experimental XRPD patterns of chlorpropamide samples are different in different reports and do not match the patterns derived from the structure.

- $\alpha$ : Several samples were crystallized from various solvents and found out to be undistinguished in XRPD patterns. For the experiments, we choose the sample with most dense powder, filling a crucible with the greatest mass. A single crystal was picked up for the low-temperature structure investigations (to be published). Single crystal structure data:  $a=5.230(2)$  Å,  $b=9.088(2)$  Å,  $c=26.673(6)$  Å,  $Z=4$ , orthorhombic,  $P2_12_12_1$ , calculated density  $\rho_c=1.450$  g cm<sup>-3</sup>. These data were received after single-crystal experiments. They are close to the data in [11]. XRPD pattern is in Table 1.
- $\beta$ : This polymorph of chlorpropamide was crystallized in two ways. First, we used the combination of two solvents, hexane and ethyl acetate. Hexane (2.5 mL) was poured into a cone flask with chlorpropamide (87 mg) and brought to the boil. A part of chlorpropamide remained unsolved on the bottom of the flask, and ethyl acetate was added drop by drop to the boiling solution until the sediment disappeared. Total, the hexane-to-ethyl acetate ratio turned out to be about 3–4. Then the solution was filtered hot and kept at room temperature in a sealed flask. After the cooling down to room temperature, small druses of crystals were found at the bottom of the flask. We failed to pick up a single crystal appropriate for the structure solution in that sample. The second procedure of the crystallization was like the first one, except that heptane was used instead of hexane as a co-solvent. Now the product was a white powder consisting of

**Table 1** X-ray powder diffraction pattern of  $\alpha$ -chlorpropamide

$h$	$k$	$l$	$d_{\text{exp}}/\text{Å}$	$I/I_0/\%$
0	0	2	13.2915	25
0	1	2	7.5149	73
0	0	4	6.6699	2
0	1	4	5.3782	2
1	0	1	5.1393	1
1	0	2	4.8761	10
0	2	0	4.5533	100
1	1	1	4.4586	3
0	0	6	4.4482	10
*1	1	2	4.3001	10
1	0	4	4.1194	86
*1	1	3	4.0443	22
*0	1	6	3.9899	5
1	1	4	3.7481	39
1	0	5	3.7376	37
1	1	5	3.4534	38
1	2	1	3.3973	10
1	2	2	3.3236	22
1	2	3	3.2061	7
*1	1	6	3.1761	35
0	1	8	3.1294	2
1	0	7	3.0838	19
1	2	4	3.0517	21
0	3	2	2.9550	4
*1	1	7	2.9191	24
1	2	5	2.8855	5
0	1	9	2.8172	4

small transparent plates, fractions of millimeter in size, suitable for single-crystal X-ray diffraction analysis [12]. Single crystal structure data:  $a=14.777(3)$  Å,  $b=9.316(4)$  Å,  $c=19.224(5)$  Å,  $Z=8$ , orthorhombic,  $Pbcn$ ,  $\rho_c=1.389$  g cm<sup>-3</sup>. XRPD pattern is in Table 2.

- $\gamma$ : Sample was crystallized from a mixture of heptane and ethyl acetate (1:2), with 300 mg of starting chlorpropamide and 110 mg of the product. Crystallization was carried out by freezing ( $-20^\circ\text{C}$ ). Sample preparation was described elsewhere [13]. Single crystal structure data:  $a=6.126(2)$  Å,  $b=8.941(6)$  Å,  $c=12.020(4)$  Å,  $\beta=99.68(3)^\circ$ ,  $Z=2$ , monoclinic,  $P2_1$ ,  $\rho_c=1.416$  g cm<sup>-3</sup>. XRPD pattern is in Table 3.
- $\delta$ : Sample was crystallized from a mixture of heptane (1 mL) and ethyl acetate (0.5 mL), with 65 mg of starting chlorpropamide and 45 mg of the product. Several single crystals were picked up for the structure solution. Unfortunately, all the crystals were

**Table 2** X-ray powder diffraction pattern of  $\beta$ -chlorpropamide

<i>h</i>	<i>k</i>	<i>l</i>	$d_{\text{exp}}/\text{\AA}$	$I/I_0/\%$
0	0	2	9.6103	11
1	0	2	8.0497	37
1	1	0	7.8831	34
1	1	1	7.2969	36
1	1	2	6.0969	7
2	1	1	5.5491	5
0	0	4	4.8111	100
0	2	0	4.6562	6
1	0	4	4.5756	27
0	2	1	4.5385	39
3	1	0	4.3573	51
3	1	1	4.2575	18
*1	2	2	4.0358	26
2	2	0	3.9494	10
0	2	3	3.7734	18
*4	0	0	3.6986	10
4	0	2	3.4503	12
4	1	1	3.3843	7
1	2	4	3.2620	22
4	1	2	3.2341	29
*0	0	6	3.2025	80
1	0	6	3.1274	5
*1	3	0	3.0409	7
*4	1	3	3.0263	10
2	0	6	2.9401	8
5	0	2	2.8274	10
*4	1	4	2.7930	10
*2	3	2	2.7448	6

\*several overlapping reflections

of low quality, and the cif-files do not meet the requirements for the publication in Acta Crystallographica. We failed to prepare a good crystal so far. Nevertheless, the structure was solved, and this allows us to analyze the arrangement of molecules and the conformation of the molecule itself, to index the XRPD pattern, and to generate the pattern identical with the experimental one. Single crystal structure data:  $a=9.32(2)$  Å,  $b=10.35(1)$  Å,  $c=26.29(3)$  Å,  $Z=8$ , orthorhombic,  $Pbca$ ,  $\rho_c=1.450$  g cm<sup>-3</sup>. Unit cell parameters after powder diffraction:  $a=9.34(1)$  Å,  $b=10.34(1)$  Å,  $c=26.30(2)$  Å. XRPD pattern is in Table 4.

- $\epsilon$ : Sample was prepared from a powder of  $\alpha$ -polymorph after the solid-solid transformation near the melting point. We failed to crystallize it from a solution. The product is a powder not suitable

**Table 3** X-ray powder diffraction pattern of  $\gamma$ -chlorpropamide

<i>h</i>	<i>k</i>	<i>l</i>	$d_{\text{exp}}/\text{\AA}$	$I/I_0/\%$
0	0	1	11.8168	13
0	1	1	7.1483	51
1	0	0	6.0554	8
-1	0	1	5.7977	60
1	1	0	5.0158	7
0	1	2	4.9457	14
-1	1	1	4.8745	5
-1	0	2	4.6441	48
0	2	0	4.4807	46
1	1	1	4.4035	64
0	2	1	4.1804	7
-1	1	2	4.1197	45
0	0	3	3.9571	35
1	0	2	3.9188	31
*1	1	2	3.5930	100
-1	2	1	3.5419	13
1	2	1	3.3436	19
-1	1	3	3.3333	24
-1	2	2	3.2210	8
1	0	3	3.0762	63
-2	0	1	3.0528	11
*0	2	3	2.9618	33
1	2	2	2.9422	4
1	1	3	2.9098	7
-2	0	2	2.8972	17
*-2	1	1	2.8877	6
*-1	0	4	2.8584	6
-1	2	3	2.8061	9
2	1	1	2.6857	10
-2	0	3	2.6217	6
1	3	1	2.5663	7
1	2	3	2.5348	10
-2	1	3	2.5154	3
0	2	4	2.4695	2
-2	2	2	2.4319	2

\*several overlapping reflections

for the single-crystal structure solution. Structure of this polymorph is unknown so far. Unit cell parameters were defined after XRPD experiments. Structure data (powder diffraction):  $a=7.360(7)$  Å,  $b=9.16(1)$  Å,  $c=19.93(1)$  Å,  $Z=4$ , orthorhombic,  $\rho_c=1.368$  g cm<sup>-3</sup>. XRPD pattern is in Table 5.

**Table 4** X-ray powder diffraction pattern of  $\delta$ -chlorpropamide

<i>h</i>	<i>k</i>	<i>l</i>	$d_{\text{exp}}/\text{\AA}$	$I/I_0/\%$
0	0	2	13.1064	67
1	0	2	7.6186	37
1	1	1	6.7082	6
0	0	4	6.5791	12
1	1	2	6.1402	9
1	0	4	5.3763	3
1	1	4	4.7805	5
2	0	0	4.6717	6
*0	2	3	4.4571	83
*0	0	6	4.3891	21
2	1	0	4.2559	51
*1	1	5	4.1919	8
2	1	2	4.0409	3
1	2	3	4.0173	4
1	0	6	3.9728	3
2	1	3	3.8338	68
1	2	4	3.7239	8
1	1	6	3.7058	7
0	2	5	3.6881	6
*1	2	5	3.4313	16
*0	2	6	3.3431	100
1	1	7	3.3008	7
1	2	6	3.1509	4
2	2	4	3.0658	6
0	2	7	3.0393	4
*1	3	4	2.9021	6
*1	2	7	2.8921	14
*2	1	7	2.8152	4
*2	3	0	2.7724	15
*3	1	4	2.7112	3
2	0	8	2.6868	4
0	0	10	2.6288	4
1	0	10	2.5314	7
*0	4	3	2.4799	8
*1	3	7	2.4525	5
*2	3	6	2.3446	17
*1	2	10	2.2732	9

**Table 5** X-ray powder diffraction pattern of  $\varepsilon$ -chlorpropamide

<i>h</i>	<i>k</i>	<i>l</i>	$d_{\text{exp}}/\text{\AA}$	$I/I_0/\%$
0	0	2	9.9636	1
1	0	1	6.9040	45
0	1	2	6.7341	24
1	0	2	5.9171	33
1	1	1	5.5104	1
*0	0	4	4.9817	7
0	2	0	4.5826	8
1	1	3	4.3463	72
1	0	4	4.1263	100
*1	1	4	3.7643	15
*1	2	2	3.6221	2
1	0	5	3.5049	21
*2	1	1	3.3671	10
0	0	6	3.3201	5
1	1	5	3.2725	22
2	0	3	3.2190	20
0	1	6	3.1233	11
1	2	4	3.0652	5
1	0	6	3.0286	15
2	0	4	2.9686	35
1	1	6	2.8754	9
2	2	0	2.8684	7
2	2	1	2.8387	3
1	2	5	2.7837	5
0	2	6	2.6883	3
1	0	7	2.6564	5
*1	3	3	2.5959	2
1	1	7	2.5518	3
0	0	8	2.4909	6
2	0	6	2.4662	6
0	1	8	2.4015	1
2	1	6	2.3815	5
2	2	5	2.3302	3
*3	0	3	2.3013	6
*1	1	8	2.2861	7

\*several overlapping reflections

### Methods

#### Powder diffraction

X-ray powder diffraction (XRPD) patterns were measured using D8 GADDS of Bruker AXS ( $\text{CuK}\alpha$  radiation,  $\lambda=1.5418$  Å, graphite monochromator,

collimator 0.5 mm, area detector Hi-Star) over the range of  $2\theta$  angles from 5 to 45°. Data were evaluated using software EVA and TOPAS P. XRPD pattern of  $\varepsilon$ -chlorpropamide was indexed using algorithm TREOR built in the software WIN-INDEX. Unit cell parameters were refined using WIN-METRIC. All programs are from the software kit of Bruker AXS GmbH (1998–2000). XRPD patterns for all poly-

morphs are listed in the Tables. Unit cell parameters after XRPD are equal to those after single-crystal diffraction within the limits of experimental errors.

### Single-crystal diffraction

Data collection was done with a Stoe STADI4 4-circle-diffractometer D094 (MoK $\alpha$  radiation,  $\lambda=0.71073$  Å, graphite monochromator, scintillation counter). Unit cell parameters for  $\beta$ -polymorph were refined using 24 reflections in the range of  $2\theta$  from 16 to 22°. Data collection for two unique sets was performed in the range of  $2\theta$  from 3 to 50°, with average  $I/\sigma$  value of 1.2. Crystal destroyed by the end of the experiment, making the data impossible to be improved. The structure was solved and refined by using SHELX-97 [16]. Structure was refined to the value of  $R=0.187$ . Anisotropic displacement parameters were calculated not for all non-hydrogen atoms. Atomic coordinates for  $\delta$ -chlorpropamide are listed in Table 6.

**Table 6** Atomic coordinates in  $\delta$ -chlorpropamide after single-crystal structure solution ( $a = 9.32(2)$  Å,  $b = 10.35(1)$  Å,  $c = 26.29(3)$  Å, Sp.gr. *Pbca*)

Atom	$x/a$	$y/b$	$z/c$
C1	0.161(3)	0.645(3)	0.293(1)
C2	0.048(3)	0.729(3)	0.298(1)
C3	0.042(3)	0.810(3)	0.3404(9)
C4	0.148(2)	0.802(2)	0.3772(7)
C5	0.261(3)	0.715(2)	0.3694(8)
C6	0.271(3)	0.634(3)	0.3282(9)
C7	0.158(3)	0.728(3)	0.500(1)
C8	0.135(3)	0.546(3)	0.5632(9)
C9	0.112(5)	0.566(4)	0.619(1)
C10	0.142(5)	0.683(4)	0.638(1)
N1	0.071(2)	0.818(2)	0.4734(8)
N2	0.072(2)	0.645(2)	0.5309(7)
O1	0.014(2)	0.994(2)	0.4202(6)
O2	0.270(2)	0.947(2)	0.4405(6)
O3	0.284(2)	0.724(2)	0.5011(7)
C11	0.177(2)	0.542(1)	0.2420(4)
S1	0.1311(8)	0.9055(8)	0.4293(3)

### Differential scanning calorimetry

Calorimetric measurements were carried out using DSC-204 Netzsch with standard aluminum crucibles of 0.04 mL in a flow of dry argon of 15 mL min $^{-1}$ . DSC was used both for the measurements of heat effects and for the preparation of  $\epsilon$ -polymorph. To define the polymorph after a heat event, the experiment was interrupted and the sample was analyzed by XRPD. The crucibles were not sealed.

Accuracy of calorimetric signal measurements was about  $\pm 2\%$ , but the accuracy of the enthalpy of transitions was significantly less because of the uncertainty in the baseline.

### Thermogravimetry

Thermogravimetric experiments were carried out using TG-209 Netzsch in an open aluminum crucible of 0.3 mL in a flow of dry argon of 20 mL min $^{-1}$ . Sample holder of the TG is equipped with a temperature sensor, which allows one to calculate (estimate) the heat flow during the experiment (c-DTA technique).

## Results and discussion

### Evaporation

Results of thermogravimetric experiments of  $\alpha$ -chlorpropamide are shown in Fig. 1. Sample mass is 16.2 mg, heating rate 12°C min $^{-1}$ . The mass remains constant at the heating up to about 140°C. Then, the evaporation starts and increases exponentially with temperature. Signal of c-DTA shows the endothermic melting (double peak, starts near 123°C) and then the irregular changes in the heat flow. Signal decreases after the peak, and then increases again due to the evaporation, together with the derivative of TG. One can conclude from these results that the contribution to the heat flow from the evaporation is negligible below 135°C.

### DSC of $\alpha$ -polymorph

Calorimetric results for  $\alpha$ -chlorpropamide are shown in Fig. 2. Double 'melting' peak at a heating rate of 6°C min $^{-1}$  indicates complex process. Study of polymor-

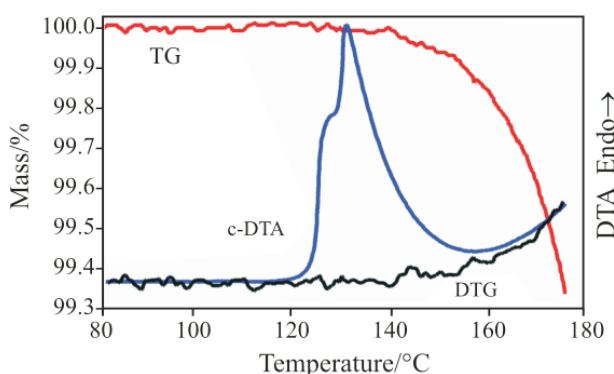


**Fig. 1** Thermogravimetric results for  $\alpha$ -chlorpropamide. c-DTA peak is the melting. Evaporation contribution (seen in TG and DTG curves) to the heat flow is negligible below 140°C

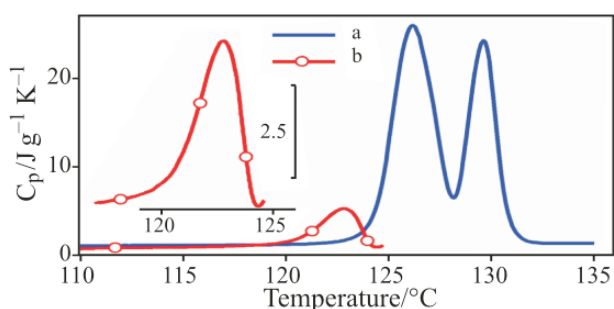


**Fig. 2** Heat capacity of  $\alpha$ -chlorpropamide near the melting point measured at fast (a –  $6^{\circ}\text{C min}^{-1}$ ) and slow (b –  $1^{\circ}\text{C min}^{-1}$ ) heating

phism from DSC melting curves with double and multiple peaks was described in [17]. We do not use here the technique of fitting the experimental data to a set of separate peaks and evaluate the total enthalpy instead.

It was published in literature that the  $\alpha$ -chlorpropamide transforms at heating into another polymorph, termed C-polymorph (A to C transition) [4]. One should remember that the letter notification is not identical with the same letters in [1]. This polymorph transition is kinetic in nature, and a slow heating can complete it significantly below the melting point. Results of the measurements at a heating rate of  $1^{\circ}\text{C min}^{-1}$  are shown also in Fig. 2. Now the first peak has finished near  $124^{\circ}\text{C}$ . At  $6^{\circ}\text{C min}^{-1}$  it was only the start of the endothermic effect. The heating was interrupted, and the sample was analyzed by X-ray diffraction. It was pure  $\varepsilon$ -polymorph. Total enthalpy of the double peak at the fast heating was  $99\text{ J g}^{-1}$ , and the enthalpy of the peak at the slow heating was  $11\text{ J g}^{-1}$ .

#### DSC of $\beta$ -polymorph

Calorimetric results for  $\beta$ -chlorpropamide are shown in Fig. 3. Peak is single at a heating rate of  $6^{\circ}\text{C min}^{-1}$  (fast heating). It starts at  $126.8^{\circ}\text{C}$ . For slow heating ( $1^{\circ}\text{C min}^{-1}$ ), the peak starts at  $125.6^{\circ}\text{C}$ , and a small satellite peak appears at the end of the process.

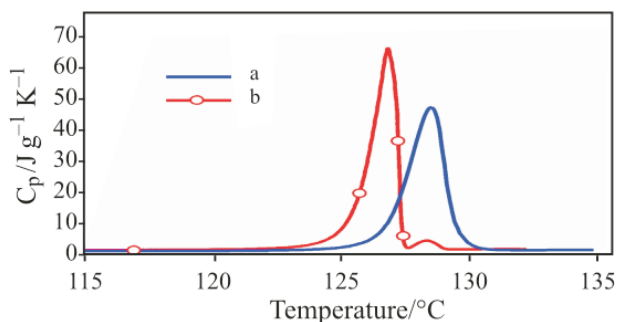


**Fig. 3** Heat capacity of  $\beta$ -chlorpropamide near the melting point measured at fast (a –  $6^{\circ}\text{C min}^{-1}$ ) and slow (b –  $1^{\circ}\text{C min}^{-1}$ ) heating

Enthalpies of the transition in both experiments are very close to each other:  $84$  and  $85\text{ J g}^{-1}$ . The difference is within the limits of experimental error.

There are two variants to describe the results of the slow heating: (1) two endothermic peaks (processes) run in a series one by one; (2) large endothermic and small exothermic peaks overlap with one another, forming a double-humped curve. As for the first variant, we do not know the nature of the second endothermic peak. It is to be the process in the melt. It is quite unusual to detect the phase transitions in liquids. We prefer the second variant, with endothermic and exothermic processes. Endothermic process is the melting and exothermic one is the polymorph transition  $\beta \rightarrow \varepsilon$  during the melting. It is like the double peaks at fast heating for  $\alpha$ - and  $\delta$ -polymorphs (see below), but with the two peaks very different in magnitude. This polymorph transition after long heating at  $60^{\circ}\text{C}$  was reported in [18]. In our experiments, it is supported by IR spectroscopy of all chlorpropamide polymorphs near the melting point. Spectrum of  $\beta$ -polymorph changes first to that of  $\varepsilon$ -polymorph, and then to the spectrum of liquid chlorpropamide. Spectroscopic results will be published in a separate report.

#### DSC of $\gamma$ -polymorph

Calorimetric results for  $\gamma$ -chlorpropamide are shown in Fig. 4. Unusual thermal effect occurs near  $120^{\circ}\text{C}$  at a heating rate of  $6^{\circ}\text{C min}^{-1}$ . It starts with endothermic process and finishes with exothermic one. Heat production is large enough to heat the sample up (negative heat capacity). We repeated the experiment at a heating rate of  $3^{\circ}\text{C min}^{-1}$ . The effect appeared at a less temperature and with a less magnitude. Now exothermic heat effect does not heat the sample up, heat capacity remains positive. The measurement was stopped just after the finish of the exothermic part, and the sample was analyzed by X-ray diffraction. It transforms into pure  $\varepsilon$ -polymorph. Total enthalpy of all peaks (polymorph transition+melting) at the fast heating was  $92\text{ J g}^{-1}$ .

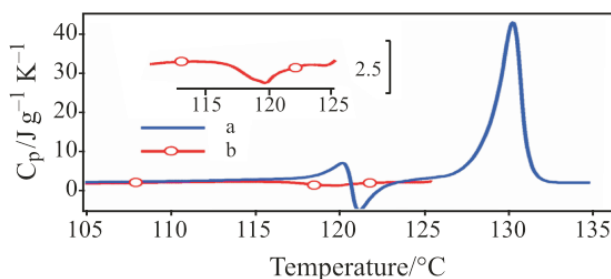


**Fig. 4** Heat capacity of  $\gamma$ -chlorpropamide near the melting point measured at fast (a –  $6^{\circ}\text{C min}^{-1}$ ) and slow (b –  $3^{\circ}\text{C min}^{-1}$ ) heating

### DSC of $\delta$ -polymorph

Calorimetric results for  $\delta$ -chlorpropamide are shown in Fig. 5. We see again a double 'melting' peak at a heating rate of  $6^\circ\text{C min}^{-1}$ , like it was for  $\alpha$ -chlorpropamide. There is a minimum at  $127.5^\circ\text{C}$  between two peaks, at  $126$  and  $129.5^\circ\text{C}$ . Heat capacity at the minimum is less than the baseline value (shown in the Figure by the dotted line), indicating an exothermic contribution in the bulk process. We repeated the experiment at a heating rate of  $1^\circ\text{C min}^{-1}$  and found out that the exothermic contribution manifested itself evidently. The heating was stopped at  $124^\circ\text{C}$  and the sample was analyzed by X-ray diffraction. It turned out to be the pure  $\varepsilon$ -polymorph. Total enthalpy of the double peak at the fast heating was  $87\text{ J g}^{-1}$ .

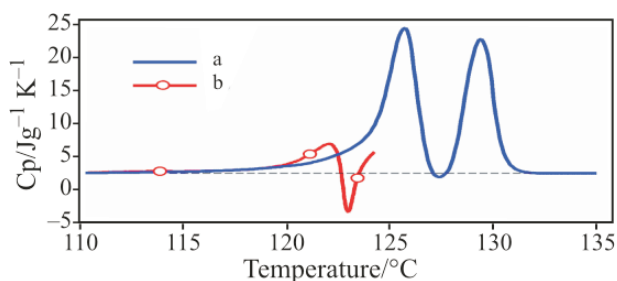


**Fig. 5** Heat capacity of  $\delta$ -chlorpropamide near the melting point measured at fast (a –  $6^\circ\text{C min}^{-1}$ ) and slow (b –  $1^\circ\text{C min}^{-1}$ ) heating

### DSC of $\varepsilon$ -polymorph

Calorimetric results for  $\varepsilon$ -chlorpropamide at a heating rate of  $3^\circ\text{C min}^{-1}$  are shown in Fig. 6. Slow-heating ( $0.3^\circ\text{C min}^{-1}$ ) experiment with the  $\alpha$ -chlorpropamide for the sample preparation is also shown in the Figure.  $\varepsilon$ -chlorpropamide melts at  $128^\circ\text{C}$  with the enthalpy of  $87\text{ J g}^{-1}$ .

### Completeness of the list of chlorpropamide polymorphs

Today the structure of four polymorphs of chlorpropamide ( $\alpha$ ,  $\beta$ ,  $\gamma$ ,  $\delta$ ) and the unit cell parameters of the fifth one ( $\varepsilon$ ) are known. Having their XRPD patterns (shown in Fig. 7), we examined the literature data and found out that polymorphs  $\alpha$ ,  $\beta$ ,  $\gamma$  and  $\varepsilon$  were prepared elsewhere, in mixture or in pure form. On the other hand, all published XRPD patterns of chlorpropamide can be described only with these four polymorphs. Polymorph  $\delta$  was received never before. Thus, today one may consider this list of five chlorpropamide polymorphs prepared under ambient conditions complete.

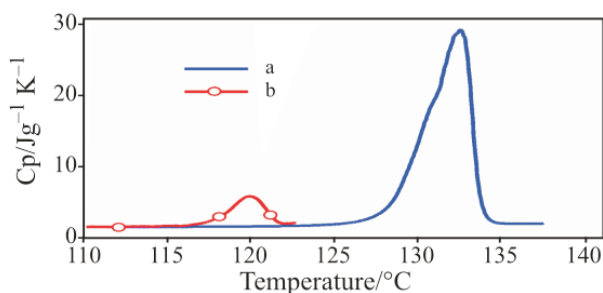


**Fig. 6** Heat capacity of  $\varepsilon$ -chlorpropamide near the melting point measured at a heating rate of a –  $3^\circ\text{C min}^{-1}$ . The sample was prepared during the polymorph transition  $\alpha \rightarrow \varepsilon$  at a heating rate of b –  $0.3^\circ\text{C min}^{-1}$

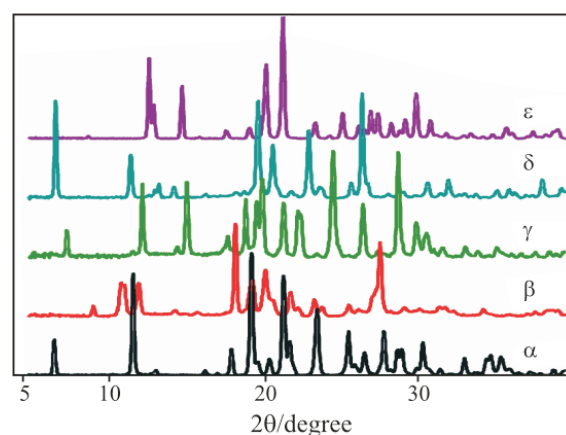


**Fig. 7** XRPD patterns of five polymorphs of chlorpropamide

### Enthalpy of polymorph transitions

Melting of  $\alpha$ ,  $\beta$ ,  $\gamma$  and  $\delta$  polymorphs is accompanied with the transformation into  $\varepsilon$ -polymorph. Enthalpy measured in the experiment consists of two contributions, enthalpy of polymorph transition  $\Delta_{tr}H$  and the enthalpy of melting of  $\varepsilon$ -polymorph  $\Delta_mH(\varepsilon)$ . For  $\alpha$ -polymorph, for example, we have

$$\Delta H(\alpha) = \Delta_{tr}H(\alpha \rightarrow \varepsilon) + \Delta_mH(\varepsilon)$$

Using the measured values of total enthalpy of melting in the fast heating experiments for each polymorph and the enthalpy of melting for  $\varepsilon$ -polymorph, we have the enthalpy of the polymorph transition  $12\text{ J g}^{-1}$  for  $\alpha$ ,  $-3\text{ J g}^{-1}$  for  $\beta$ ,  $5\text{ J g}^{-1}$  for  $\gamma$ , and  $0\text{ J g}^{-1}$  for  $\delta$ . Accuracy of these values is about  $\pm 3\text{ J g}^{-1}$ , considering the accuracy of calibration and the uncertainty in the baseline.

### Kinetic restrictions in the $\beta \rightarrow \varepsilon$ transition

Enthalpy of  $\alpha \rightarrow \varepsilon$  transition is the largest. Polymorph  $\alpha$  is the most stable one under ambient conditions. It crystallizes readily from various solutions and does not trans-

form into another polymorph at storage. In order of decreasing enthalpy, the next are  $\gamma$  and  $\delta$  polymorphs. Both transform into  $\varepsilon$ -polymorph, and the transformation starts with an endothermic stage, changing then to exothermic one. Heat release for  $\delta$ -polymorph is greater than that for  $\gamma$ -polymorph. This agrees again with the value of the transition enthalpy. For the  $\beta$ -polymorph, the rule is violated. Its enthalpy of transition is the least, even negative. It is most unstable, and must transform into  $\varepsilon$ -polymorph spontaneously and with the greatest heat release. But this is not the case.  $\beta$ -polymorph transforms into  $\varepsilon$ -polymorph very slowly. At scanning heating, the transition manifests itself only at slow heating at the very end of the process. Such anomalous behavior is explained by the kinetic reasons, arising from the structural difference between  $\beta$  and the rest polymorphs.

Structure of  $\alpha$ ,  $\beta$ ,  $\gamma$  and  $\delta$  polymorphs is formed by the bands of molecules. Long molecule of chlorpropamide has a benzene ring at one end, central part with a sequence of S–N–C–N atoms, participating in the hydrogen bonds, and an alkyl 'tail'. Molecules are tied by conventional hydrogen bond N–H...O inside the band and by weak van der Waals interaction between the bands. Neighbor molecules in the band arrange always oppositely, (benzene ring–core–alkyl 'tail') vs. (alkyl 'tail'–core–benzene ring). Figure 8 shows the fragment of the band, consisting of two molecules.

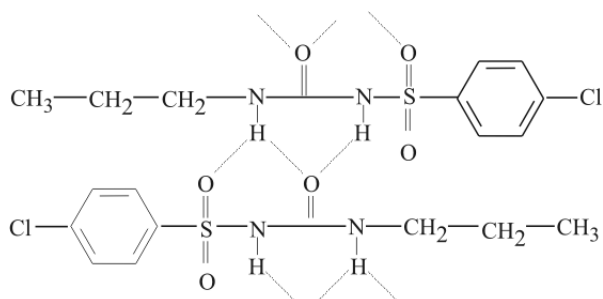


**Fig. 8** Opposite orientation of neighbor molecules in the band, forming the structure of chlorpropamide

Structures of the polymorphs differ from one another in the spatial arrangement of benzene rings and alkyl 'tails', shown in Fig. 9. Benzene rings of all molecules are on the different sides of the plane formed by molecules in a band for  $\alpha$ ,  $\gamma$  and  $\delta$ , but on the same side for  $\beta$ . Polymorph transitions among  $\alpha$ ,  $\gamma$  and  $\delta$  structures can be proceeded by the changes in the molecule conformation (rotation of a plane of the benzene ring, displacement of C atoms in the alkyl 'tail'), without significant reconstruction of the whole structure. As for the transition from  $\beta$  to the rest polymorphs, the case is completely different. Neighbor bands prevent the benzene ring (right on the Figure) from the rotation clockwise, into the position on the opposite side of the band. To overturn every second ring in a band, one need to move neighbor bands

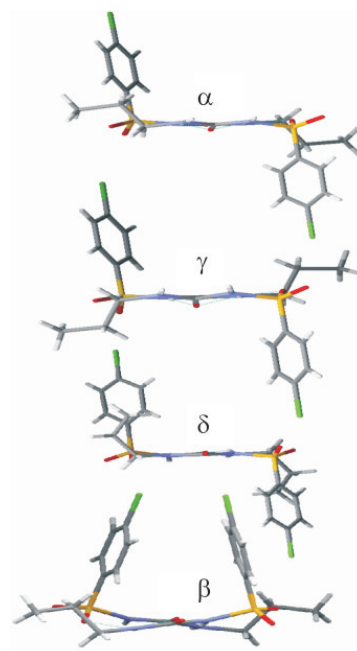


**Fig. 9** Arrangement of a pair of chlorpropamide molecules in various polymorphs. Benzene rings are on opposite sides of the band in  $\alpha$ ,  $\gamma$  and  $\delta$ , but on the same side in the  $\beta$ -polymorph

aside. It is possible during the melting. The fact that  $\alpha$ ,  $\gamma$  and  $\delta$  transform into  $\varepsilon$ -polymorph readily in a solid state, and  $\beta$  with difficulty, allows us to suppose that the structure of  $\varepsilon$ -polymorph contains the benzene rings on the opposite sides of the band's plane.

## Conclusions

Five polymorphs of chlorpropamide were investigated by DSC near the melting point. Four polymorph with known structure ( $\alpha$ ,  $\beta$ ,  $\gamma$  and  $\delta$ ) were found to transform into the fifth polymorph ( $\varepsilon$ ) with unknown structure. Enthalpy of polymorph transitions was estimated after the measurements of the sum heat effect of a melting. According to these data,  $\beta$ -polymorph is most unstable, but transition  $\beta \rightarrow \varepsilon$  is less active in the experiment. Structure of  $\beta$ -polymorph differs significantly from those of the rest polymorphs. To transform  $\beta$ -polymorph into another structure, one needs to increase the distance between neighbor bands. This stops the kinetics of polymorph transition  $\beta \rightarrow \varepsilon$ . Structure motif in  $\varepsilon$ -polymorph is similar to those in  $\alpha$ ,  $\gamma$  and  $\delta$ , and dissimilar to that in  $\beta$ .

## Acknowledgements

This work was supported by a grant from BRHE (Y3-C-08-01), a grant from the Russian Ministry of Education



and Science (2.2.2.3.2007), RFBR grant No. 05-03-32468, and Integration Projects No. 49 and 110 of the Siberian Branch of RAS.

## References

- 1 D. L. Simmons, R. J. Ranz and N. D. Guanchandani, *Can. J. Pharm. Sci.*, 8 (1973) 125.
- 2 S. S. Al-Saeq and G. R. Riley, *Pharm. Acta Helv.*, 57 (1982) 8.
- 3 H. Ueda, N. Nambu and T. Nagai, *Chem. Pharm. Bull.*, 32 (1984) 244.
- 4 C. Vemavarapu, M.J. Mollan and T.E. Needham, *AAPS PharmSciTech*; 3 (2002) article 29 (<http://www.aapspharmsci.org>).
- 5 Y. Sonoda, F. Hirayama, H. Arima and K. Uekama, *J. Incl. Phenom. Macro.*, 50 (2004) 73.
- 6 J. Bernstein, *Polymorphism in Molecular Crystals*. Oxford Univ. Press, Oxford, 2002, p. 424.
- 7 J. D. Dunitz and J. Bernstein, *Acc. Chem. Res.*, 28 (1995) 193.
- 8 R. Barbas, R. Prohens and C. Puigjaner, *J. Therm. Anal. Cal.*, 89 (2007) 687.
- 9 D. Giron, S. Monnier, M. Mutz, P. Piechon, T. Buser, F. Stowasser, K. Schulze and M. Bellus, *J. Therm. Anal. Cal.*, 89 (2007) 729.
- 10 F. N. Allen, *Acta Cryst.*, B58 (2002) 380.
- 11 C. H. Koo, S. I. Cho and Y. H. Yeon, *Arch. Pharmacol. Res.*, 3 (1980) 37.
- 12 T. N. Drebuschak, N. V. Chukanov and E. V. Boldyreva, *Acta Cryst.*, E62 (2006) o4393.
- 13 T. N. Drebuschak, N. V. Chukanov and E. V. Boldyreva, *Acta Cryst.*, C63 (2007) o355.
- 14 P. L. D. Wildfong, K. R. Morris, C. A. Anderson and S. M. Short, *J. Pharm. Sci.*, 96 (2007) 1100.
- 15 E. Yonemochi, Y. Yoshioka, Y. Yoshihashi and K. Terada, *J. Therm. Anal. Cal.*, 85 (2006) 693.
- 16 G. M. Sheldrick, (1997) SHELX97. University of Göttingen, Germany.
- 17 M. L. P. Leitão, J. Canotilho, M. S. C. Cruz, J. C. Pereira, A. T. Sousa and J. S. Redinha, *J. Therm. Anal. Cal.*, 68 (2002) 397.
- 18 M. M. De Villiers and D. E. Wurster, *Acta Pharm.*, 49 (1999) 79.

---

Received: October 9, 2007

Accepted: October 16, 2007

---

DOI: 10.1007/s10973-007-8822-0